



Aalborg Universitet

**AALBORG UNIVERSITY**  
DENMARK

## **Round-robin analysis of the RILEM TC 162-TDF-beam-bending test. Part 2 - Approximation of $d$ from the CMOD response**

Barr, B.I.G.; Lee, M.K.; Hansen, Ernst Jan de Place; Dupont, D.; Erdem, E.; Schaerlaekens, S.; Schnütgen, B.; Stang, H.; Vandewalle, L.

*Published in:*  
Materials and Structures

*Publication date:*  
2003

*Document Version*  
Accepted author manuscript, peer reviewed version

[Link to publication from Aalborg University](#)

*Citation for published version (APA):*

Barr, B. I. G., Lee, M. K., Hansen, E. J. D. P., Dupont, D., Erdem, E., Schaerlaekens, S., Schnütgen, B., Stang, H., & Vandewalle, L. (2003). Round-robin analysis of the RILEM TC 162-TDF-beam-bending test. Part 2 - Approximation of  $d$  from the CMOD response. *Materials and Structures*, 36((November)), 621-630.

### **General rights**

Copyright and moral rights for the publications made accessible in the public portal are retained by the authors and/or other copyright owners and it is a condition of accessing publications that users recognise and abide by the legal requirements associated with these rights.

- Users may download and print one copy of any publication from the public portal for the purpose of private study or research.
- You may not further distribute the material or use it for any profit-making activity or commercial gain
- You may freely distribute the URL identifying the publication in the public portal -

### **Take down policy**

If you believe that this document breaches copyright please contact us at [vbn@aub.aau.dk](mailto:vbn@aub.aau.dk) providing details, and we will remove access to the work immediately and investigate your claim.



RILEM TC 162-TDF: 'Test and design methods for steel fibre reinforced concrete'

## Round-robin analysis of the RILEM TC 162-TDF beam-bending test: Part 2 - Approximation of $\delta$ from the CMOD response

Prepared by B.I.G. Barr<sup>1</sup> and M.K. Lee<sup>1</sup>, with contributions from E.J. de Place Hansen<sup>3</sup>, D. Dupont<sup>4</sup>, E. Erdem<sup>5</sup>, S. Schaerlaekens<sup>2</sup>, B. Schnütgen<sup>5</sup>, H. Stang<sup>3</sup> and L. Vandewalle<sup>4</sup>

(1) Cardiff University, Wales

(2) Belgian Research Institute, Belgium

(3) Technical University of Denmark, Denmark

(4) Katholieke Universiteit Leuven, Belgium

(5) Ruhr-University of Bochum, Germany

**TC Membership:** Chairlady: L. Vandewalle, Belgium; Secretary: D. Nemegeer, Belgium; Members: B. Barr, UK; P. Bartos, UK; N. Banthia, Canada; E. Denarié, Suisse; M. Di Prisco, Italy; H. Falkner, Germany; R. Gettu, Spain; V. Häusler, Germany; K. Kovler, Israel; S. Mindess, Canada; H.-W. Reinhardt, Germany; P. Rossi, France; B. Schnütgen, Germany; S. Shah, USA; Å. Skarendahl, Sweden; H. Stang, Denmark; P. Stroeven, the Netherlands; R. Swamy, UK; J. Walraven, the Netherlands.

### ABSTRACT

A round robin test programme was carried out using the beam-bending test recommended by RILEM TC 162-TDF [1]. The test programme included both plain and steel fibre reinforced concrete (SFRC) beams. A detailed analysis was carried out to investigate the influence of different test configurations on measurements of the crack mouth opening displacement (CMOD). Linear elastic fracture mechanics (LEFM) and non-linear fracture mechanics (NLFM) methods were utilised to investigate the problem analytically. From the analytical studies carried out, it is proposed that the CMOD should not be measured at a distance more than 5mm from the bottom fibre of the beam. A larger distance than 5mm will cause the deviation between the measured CMOD and the true CMOD to reach an unacceptable level. A simple rigid body model has been proposed to relate the CMOD to the mid-span deflection. The NLFM analysis and experimental results were compared for both the plain and SFRC beam results and it was found that results based on the basis of CMOD can be compared to those based on deflections, for practical purposes, using the simple rigid body model. The experimental results strongly suggest that the rigid body model could be effectively applied for all the types of materials tested in the round robin test programme. In addition it was found that the conversion from CMOD to the equivalent mid-span deflection,  $\delta_e$ , revealed good agreement between the load-average mid-span deflection ( $P-\delta$ ) curve and the load-equivalent mid-span deflection ( $P-\delta_e$ ) curve especially for the SFRC specimens. It is proposed that the load-CMOD ( $P$ -CMOD) curve be used to calculate the proposed RILEM design parameters (as opposed to the  $P-\delta$  curve) via the use of a correction factor determined using the simple rigid body model.

### RÉSUMÉ

Un programme d'essais comparatifs entre laboratoires a été réalisé pour évaluer le test de poutre soumise à la flexion, comme prescrit par TC 162-TDF de la RILEM. Des poutres en béton normal et en béton de fibres métalliques (BFM) sont prises en compte dans le programme d'essais. Une étude détaillée a été effectuée pour examiner l'influence de différentes méthodes d'essai de mesures de l'ouverture d'orifice de fissure (OOF). La mécanique de fracture linéaire et non-linéaire a été utilisée pour examiner le problème d'une façon analytique. Sur base des études analytiques, on propose que l'OOF ne soit pas mesurée à une distance de plus de 5 mm de la base de la poutre. Au-delà de cette distance de 5 mm, la différence entre l'OOF mesurée et l'OOF véritable atteint un niveau inacceptable. Un modèle simple, basé sur des corps solides, est proposé pour estimer l'OOF à la flexion au centre de la poutre. L'analyse de la mécanique de fracture non-linéaire a été comparée avec les résultats expérimentaux pour les poutres en béton normal et en BFM. En pratique, on a constaté que les résultats basés sur l'OOF peuvent être comparés avec les résultats basés sur la déflection, si on utilise un modèle, basé sur des corps solides. Les résultats suggèrent clairement que le modèle, basé sur des corps solides, puisse être appliqué sur tous les matériaux testés dans le programme des essais comparatifs. En plus, la conversion entre l'OOF et la déflection équivalente au centre de la poutre ( $\delta_e$ ) a révélé une grande conformité entre le diagramme de la force en fonction de la déflection moyenne au centre de la poutre et le diagramme de la force en fonction de la déflection équivalente au centre de la poutre. Ceci est certainement le cas pour BFM. On propose que le diagramme de la force en fonction de l'OOF (contrairement au diagramme avec la force en fonction de la déflection) soit utilisé pour le calcul des paramètres de dimensionnement, proposé par la RILEM. Pour ce faire, on peut utiliser un facteur de correction, déterminé par le modèle, basé sur des corps solides.

## 1. INTRODUCTION

This paper gives an account of a detailed investigation of the relationship between the mid-span deflection,  $\delta$ , and the crack mouth opening displacement, CMOD, obtained in a round robin test programme executed by five test laboratories. The round robin test programme was carried out using the test configuration proposed by RILEM TC 162-TDF [1].

Further details of the round robin test programme are reported in a companion paper and will not be repeated here [2,3]. Essentially, the round robin test programme was executed in two phases with two concrete strengths considered. The concrete grades considered were C25/30, termed as normal strength concrete (NSC) and C70/85, termed as high strength concrete (HSC). The letter "C" indicates a characteristic compressive strength and the numerals indicate the compressive strengths in  $\text{N/mm}^2$  measured from cylinders and cubes respectively. Three types of fibres and fibre dosages were employed during the round robin programme *i.e.* Dramix 65/60 BN (for the NSC beams with  $25\text{kg/m}^3$  and  $75\text{kg/m}^3$  of fibres), Dramix 80/60 BN (for the NSC beams with  $50\text{kg/m}^3$  of fibres) and Dramix 80/60 BP (for the HSC beams with  $25\text{kg/m}^3$  of fibres). Plain concrete beams were also included as part of the test programme to play the role of control specimens and were a means of investigating the strengths, limitations and sensitivity of the proposed test method, as they do not contain the variations introduced by fibre distribution and orientation.

Five testing laboratories were involved in the beam bending round robin programme, with Cardiff University (UWC) as the task co-ordinator. The laboratories are (in alphabetical order):

CSTC – Belgian Building Research Institute  
 DTU – Technical University of Denmark  
 KUL – Katholieke Universiteit Leuven  
 RUB – Ruhr-University of Bochum  
 UWC – Cardiff University (task co-ordinator)

The above acronyms for each participating laboratory will be used henceforth.

## 2. RESEARCH SIGNIFICANCE

The test method advanced by the RILEM TC 162-TDF is a notched beam under three-point bending which is shown schematically in Fig. 1. From the experience gained from the round robin test programme, it was concluded that the test would be more stable if executed under CMOD control particularly for specimens with a high strength matrix. It is anticipated that the CMOD would be measured at a certain distance away from the bottom surface of the beam. Knife-edges (or other similar devices) could be used to hold the clip gauge (or LVDT in some cases) in place. The knife-edges would have a certain thickness,  $d_0$ , as illustrated in Fig. 1. The measured CMOD would have a systematic error relative to the true CMOD, with the deviation proportional with respect to some function of the thickness  $d_0$ . It is thus essential to limit the thickness of the knife-edge to a certain range to avoid unacceptably large deviations.

The test method is closely related to the  $\sigma$ - $\epsilon$  method proposed by the RILEM TC-TDF [4]. The test method requires that measurements be made of the mid-span deflections on both sides of the beam,  $\delta_1$  and  $\delta_2$ , in addition

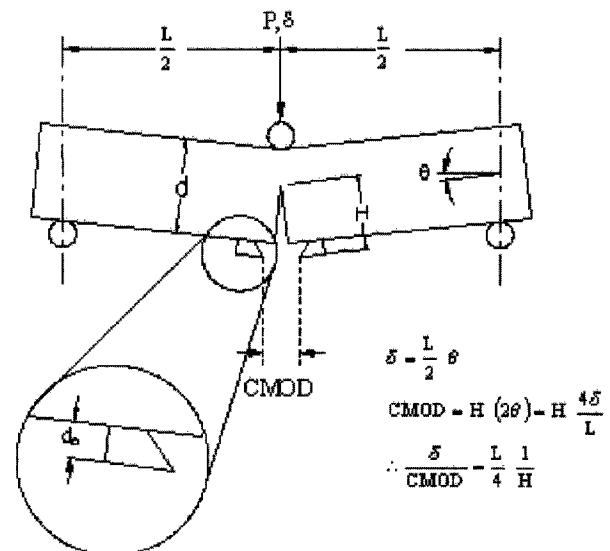


Fig. 1 – Schematic illustration showing knife-edges (or similar devices) having a certain thickness,  $d_0$ .

to the CMOD. Strictly speaking, the RILEM TC-TDF design parameters should be calculated from the load-average mid-span deflection,  $P$ - $\delta$ , curves. However, there may be certain times where this is not possible. Either, one or both deflection measurements may be found to be erroneous and this would eliminate the possibility of carrying out calculations based on the  $P$ - $\delta$  curves. Another scenario which may arise, is that some researchers may desire to carry out the tests "indirectly" by measuring only CMOD. Additionally, the possibility of obtaining all necessary design parameters from the load-CMOD ( $P$ -CMOD) curves would appeal to the practising engineer as it reduces set-up time and cost. A model relating the CMOD measurements to the mid-span deflections would pave the way to such a possibility.

The idea of using the  $P$ -CMOD curve is not a new one. Gopalaratnam *et al.* [5] found that CMOD are less prone to errors than beam deflection measurements and postulated that the  $P$ -CMOD curve could be a possible alternative measure of toughness. Also, Gopalaratnam *et al.* [6] demonstrated that there was virtually a linear relationship between mid-span deflection response and CMOD and suggested that the two could be related, for all practical purposes, using a simple relation. Barr *et al.* [7] concluded that the  $P$ -CMOD curve would be a good basis for use in the measurement of toughness and carrying out tests on notched beams via CMOD control leads to a stable post-peak response. More recently, Navalurkar *et al.* [8] proposed that the  $P$ -CMOD curve be used, instead of the  $P$ - $\delta$  curve, to evaluate the fracture energy of concrete.

## 3. CORRELATION BETWEEN CMODs AT DIFFERENT DEPTH, $d_0$

### 3.1 Scope of study

This section gives an account of a study to investigate the error introduced by using different knife-edges (or similar devices to measure/control CMOD) with different

thickness,  $d_0$ . In a beam test, the CMOD is typically measured at a fixed distance from the bottom of the beam. It is unusual to measure CMOD directly from the bottom fibre of the beam. This introduces a fixed amount of systematic error into the measured or nominal value of CMOD (defined by CMOD in Fig. 2) relative to the actual value at the beam surface *i.e.* CMOD<sup>a</sup> in Fig. 2, with the magnitude of the error increasing with an increase in the thickness of the knife-edge ( $d_0$ ).

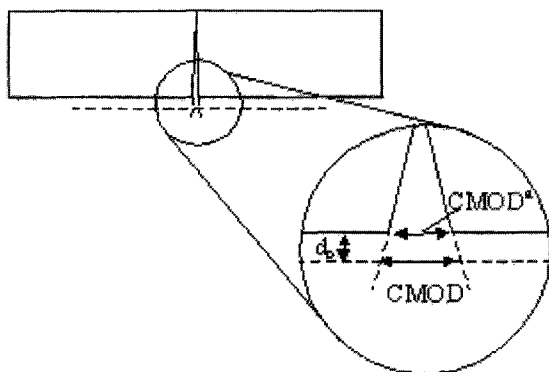


Fig. 2 – Illustration of difference between CMOD and CMOD<sup>a</sup>.

Two analytical methods were used to investigate this issue; Ferreira *et al.* [9] used linear elastic fracture mechanics (LEFM) whereas Stang [10] used non-linear fracture mechanics (NLFM). Errors introduced in terms of the difference in the CMOD measured using a certain knife-edge thickness,  $d_0$ , with that of the CMOD measured exactly at the bottom of the beam was studied. The “real” CMOD<sup>a</sup> and the nominal value, CMOD, as obtained experimentally are related as follows:

$$\text{CMOD}^a = c_c \text{CMOD} \quad (1)$$

where  $c_c$  is the theoretical correction factor for converting the measured value to the “real” CMOD.

### 3.2 Proposal for a limit to $d_0$

From the study using LEFM [9], it was found that for a knife-edge thickness of 10 mm, the error varies from values of 20% to 8% as a function of mid-span deflection. By assuming a maximum error of 5%, the study showed that a knife-edge should not have a thickness of more than 2.5 mm. For an error level of approximately 10%, the study suggests that a knife-edge should not have a thickness greater than 5 mm.

The analysis using NLFM [10] showed similar results with the error increasing with increasing knife-edge thickness. By considering knife-edge thicknesses of 2 mm and 5 mm, several correction factors were obtained for various mid-span deflections. The results are shown in Table 1. It can be observed that after a certain mid-span deflection, the correction factor approaches a constant value.

In essence, both analytical studies showed that the error introduced increases with an increase in the height of the knife-edge used and that the correction factor,  $c_c$ , varies as the test progresses. However, the change in the value of  $c_c$  is insignificant when the test is in the post-cracked phase. It is proposed that the knife-edge (or similar devices) thickness is limited to a maximum value of 5 mm. This thickness is not too small thereby making it relatively easy to fabricate with reasonable accuracy and would not be too cumbersome to handle, especially for practising engineers.

## 4. CORRELATION BETWEEN $\delta$ AND CMOD

### 4.1 Methodology

This section gives an account of an investigation to determine whether there is a simple correlation between the mid-span deflection,  $\delta$ , and the crack mouth opening displacement, CMOD. This is to enable calculations of the RILEM TC 162-TDF design parameters from P-CMOD curves to be considered as a parallel or alternative method of analysis.

In the post-cracked phase, using rigid body kinematics, it can be shown that theoretically the average mid-span deflection,  $\delta$ , can be related to CMOD. The only variable that one may encounter will be the value of  $d_0$ , which is defined in Fig. 1.

The equation relating  $\delta$  to CMOD is as follows:

$$\frac{\delta}{\text{CMOD}} = \frac{L}{4} \cdot \frac{1}{H} \quad (2)$$

where,  $L$  = span at which the beam is tested and  $H$  = the apparent depth about which the beam rotates

Equation (2) implies that the ratio of  $\delta/\text{CMOD}$  is a constant given by  $L/4$ , multiplied by the value  $1/H$ . The only problem left is to evaluate the value of  $H$ . The point at which the beam rotates can be assumed (as a first approximation) to be at the very top surface of the beam. In the case of the round robin tests,  $H$  is then estimated to be  $150 + d_0$ . In the following sections, the nominal values of CMOD (*i.e.* CMOD in Fig. 2) will be used for the analyses and should not be confused with CMOD<sup>a</sup>.

In the first phase of the round robin programme, the test labs used different values of  $d_0$  in the work carried out. Thus, the CMOD results for the plain normal strength concrete beams, C25/30, and normal strength concrete with a fibre content of 50 kg/m<sup>3</sup> was obtained via the use of different values of  $d_0$ . This gives test data to investigate the assumptions implied in Equation (2). Table 2 tabulates the values of  $d_0$  adopted by the various testing labs during the first phase of the round robin test programme.

By plotting  $\delta/\text{CMOD}$  against  $1/H$ , and by carrying out linear regression with the estimated regression line passing through the origin, one can evaluate the accuracy of the

Table 1 – Correction factors at various mid-span deflections (from non-linear fracture mechanics analysis)

$d_0$ (mm)	Correction factor, $c_c$ , at prescribed mid-span deflection									
	0.1	0.5	1.0	1.5	2.0	2.5	3.0	3.5	4.0	4.5
2	0.9733	0.9837	0.9852	0.9858	0.9862	0.9864	0.9865	<b>0.9865</b>	0.9866	0.9866
5	0.9357	0.9603	0.9639	0.9653	0.9661	0.9666	0.9668	<b>0.9670</b>	0.9671	0.9672

Note: Figures in **bold** indicate the prescribed mid-span deflection in millimeters

**Table 2 – Location of CMOD measurement devices at the various test labs (during the first phase of the round robin test programme)**

Testing lab	Thickness $d_0$ (mm)
CSTC*	-4
DTU	7.5
KUL	14
RUB†	0
UWC	5

Note: \* CSTC measured CMOD above the bottom fibre on both sides of the beam, † RUB measured the CMOD on both sides of the beam, at the bottom corners

model. A slope in close agreement with the theoretical value of  $L/4$  would imply that the model is applicable. Hence, the ratio of  $\delta/\text{CMOD}$  was calculated at distinct mid-span deflections,  $\delta$ , and these values are plotted against  $1/H$ . This was done for both the plain and SFRC beams. (Examples of these plots are shown later in Figs. 7 and 9.)

Strictly speaking, the model is only applicable for test results in the post-cracked phase. The actual relationship between  $\delta$  and CMOD is a function of the crack length, thus implying different  $\delta/\text{CMOD}$  ratios in the pre-cracked and post-cracked phases as illustrated in Figs. 3 and 4. For practical reasons, a constant value of  $\delta/\text{CMOD}$  is highly desirable. The pre-cracked phase is relatively short in comparison with the post-cracked phase, which justifies the use of a constant  $\delta/\text{CMOD}$  ratio. The assumption of a constant  $\delta/\text{CMOD}$  ratio should not have a significantly adverse effect, especially for SFRC beams as they are tested well into the post-cracked phase.

Apart from using the experimental results for the verification of Equation (2), a computer program developed at the Technical University of Denmark, DTU, was used in addition to the simple proposed model. The computer program together with a description of the analysis is given in reference [10]. The computer program was executed with fixed material and geometrical parameters but with different values of  $d_0$ . Similarly, the procedure of obtaining  $\delta/\text{CMOD}$  at various mid-span deflection points and plotting  $\delta/\text{CMOD}$  against  $1/H$  was carried out using the computed results obtained from the program.

## 4.2 Validity of model

If we assume the crack length is significantly large in the notched three-point bend test, the model suggests that the ratio of  $\delta/\text{CMOD}$  is constant in the post-peak region. Equation (2) also implies that the ratio of the area under P- $\delta$  to the area under P-CMOD is a constant. To test the validity of such a model, plots of  $\delta/\text{CMOD}$  against mid span deflections were carried out. Additionally, plots of the ratio of the area under the P- $\delta$  curves against the area under the P-CMOD curves were also prepared.

Figs. 5 and 6 show plots of  $\delta/\text{CMOD}$  against mid-span deflection,  $\delta$ , for plain and SFRC beams respectively. It is seen that the ratio of  $\delta/\text{CMOD}$  approaches a plateau after a certain value of mid-span deflection. In general, the constant plateau of  $\delta/\text{CMOD}$  occupies most of the post-peak region and this suggests that the assumptions behind the proposed model are valid especially within the post-peak region.

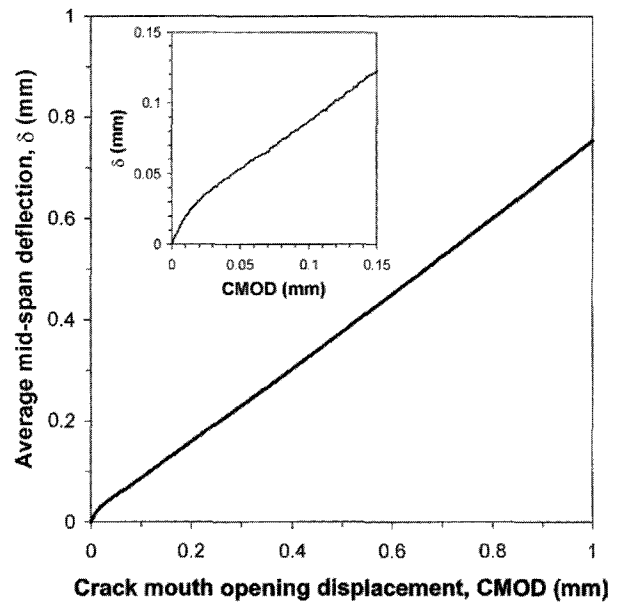


Fig. 3 – Typical plot of  $\delta$  against CMOD for a plain concrete beam with the inset figure magnifying the initial portion of the curve.

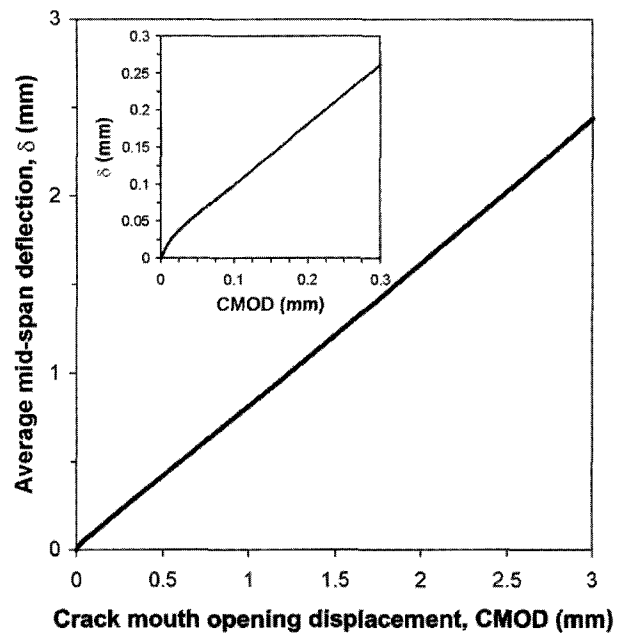


Fig. 4 – Typical plot of  $\delta$  against CMOD for a SFRC beam with the inset figure magnifying the initial portion of the curve.

Figs. 5 and 6 were plotted using the average values from all the testing labs. Thus, it is not unexpected that the plots for the NSC and HSC beams diverge from each other. This is because in the first phase of the round robin program, testing labs used very different values of  $d_0$ . On the other hand, in the second phase of the round robin, all but one used a  $d_0$  of 5 mm with the exception of RUB, who used 3 mm, but the difference is not seen to be significant.

The divergence for the SFRC beams in Fig. 6 is not as significant as seen in the plain concrete beams. This is as expected, since the SFRC beams were tested well into the post-peak region with relatively much larger mid-span deflections in comparison with the plain concrete beams.

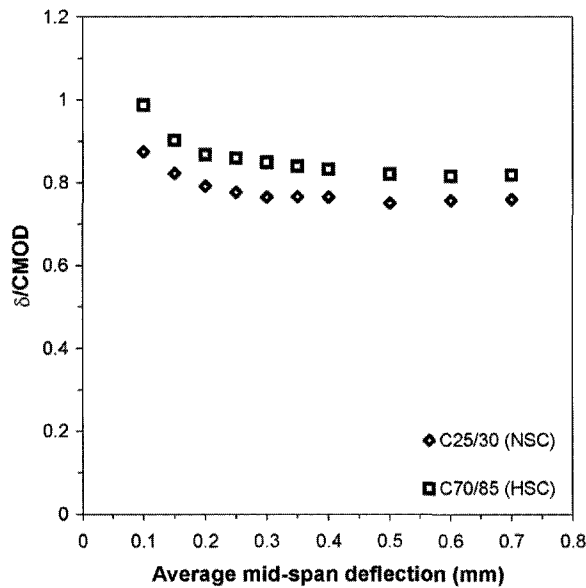


Fig. 5 – The average ratio of  $\delta/CMOD$  for plain concrete beams for a series of average mid-span deflection points.

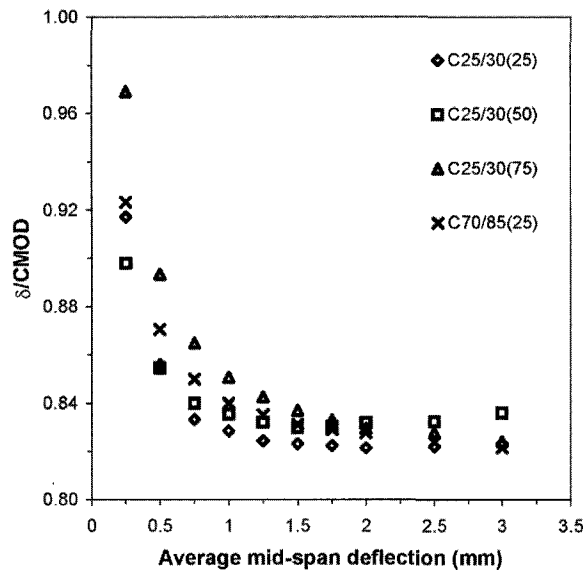


Fig. 6 – The average ratio of  $\delta/CMOD$  for SFRC beams for a series of average mid-span deflection points.

### 4.3 Results and discussion

Fig. 7 shows a plot of  $\delta/CMOD$  against  $1/H$  for a mid-span deflection of 0.4 mm for the normal strength plain concrete beams. The plot uses both the experimental results and the results computed using the aforesaid computer program from DTU. This type of plot was obtained for several mid-span deflections and the gradients were obtained by means of linear regression analysis. Although five labs were involved in the round robin programme for the beam-bending test, only four experimental data sets is available for analysis for the plain NSC specimens because all the beams in one of the labs underwent catastrophic failure.

Fig. 8 shows the gradients obtained for all average mid-span deflections considered. Both the experimental results and the analytical results are quite close to the predicted value of  $L/4$  i.e. 125 for this study. In general, it can be

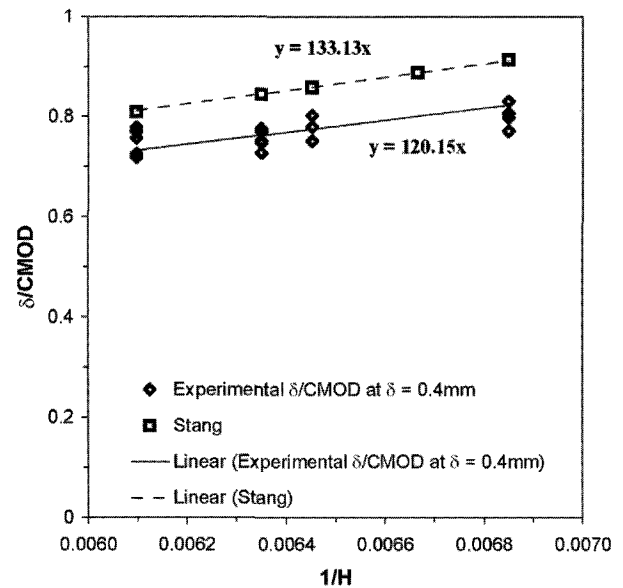


Fig. 7 – Ratio of  $\delta/CMOD$  against  $1/H$  for plain NSC beams at an average mid-span deflection of 0.4mm.

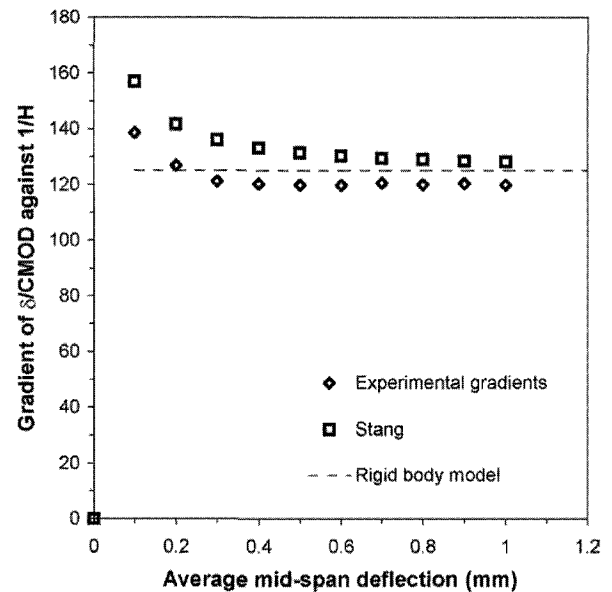


Fig. 8 – Gradients obtained at several points of mid-span deflection from experimental and analytical results for plain NSC beams.

concluded that the experimental and analytical results are in close agreement with the proposed model.

Fig. 9 shows a plot of  $\delta/CMOD$  against  $1/H$  for  $\delta = 2mm$  for the normal strength SFRC beams with a fibre content of  $50 \text{ kg/m}^3$ . Fig. 10 shows the gradients for all  $\delta$ s considered. Once again, there is close agreement between the experimental and analytical results.

### 4.4 Range of applicability

In the analysis reported in Section 4.3, consideration was only given to two types of concrete beams; the plain NSC beam and the NSC beam with a fibre content of  $50 \text{ kg/m}^3$ . A similar analysis cannot be carried out for beam results from the second phase of the round robin tests because during this phase, all but one laboratory used a  $d_o$  of 5mm. Thus a different approach was adopted to investigate whether the proposed model applies to all of the concrete types considered

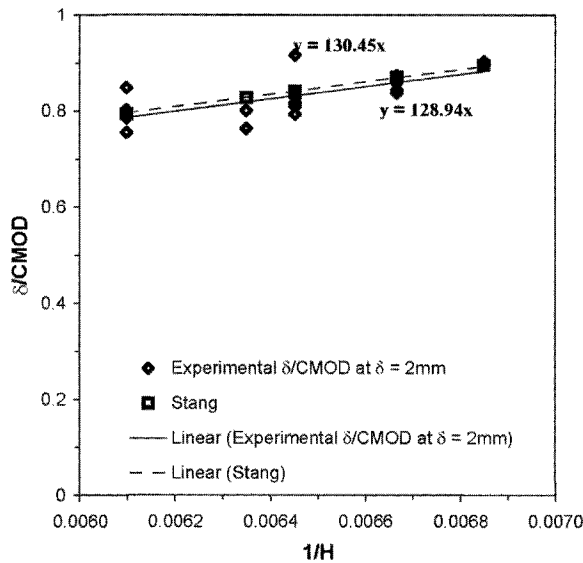


Fig. 9 – Ratio of  $\delta/CMOD$  against  $1/H$  for SFRC C25/30 (50kg/m<sup>3</sup> of fibres) at an average mid-span deflection of 2.0mm.

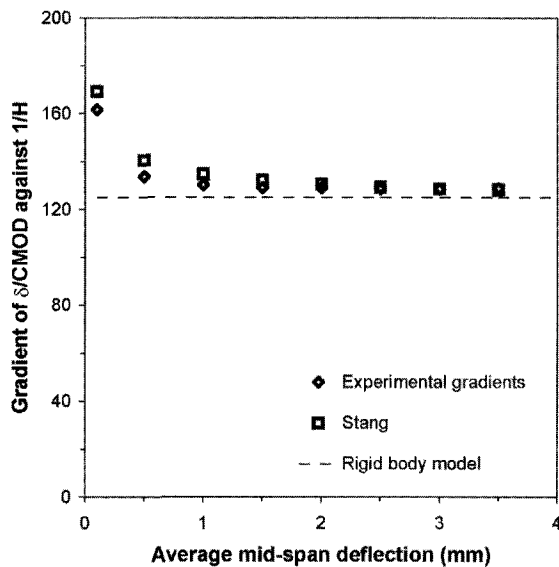


Fig. 10 – Gradients obtained at several points of mid-span deflections from experimental and analytical results for C25/30 (50kg/m<sup>3</sup> of fibres) beams.

in the round robin programme. With the confirmation that the proposed model works well with the plain concrete beams and SFRC beams from the first phase, this conclusion can be used in the analysis of the second phase beam results. This time, the CMOD at various values of  $\delta$  was obtained.

Fig. 11 shows a plot of CMOD against  $\delta$  for the plain concrete beams. It can be observed that both sets of CMOD increases in a linear manner in relation to  $\delta$ . Also, the results for NSC beams are quite close to HSC beams. Again, the divergence can be explained because of the difference in  $d_o$  adopted in the first and second phase. The plain concrete beams would be expected to be more sensitive to differences in  $d_o$  due to the fact that the tests had relatively low values of mid-span deflections.

Fig. 12 shows a plot of CMOD against  $\delta$  for the SFRC beams. Once again, the CMOD increases linearly with  $\delta$ . This time, the agreement between all the SFRC beam types is

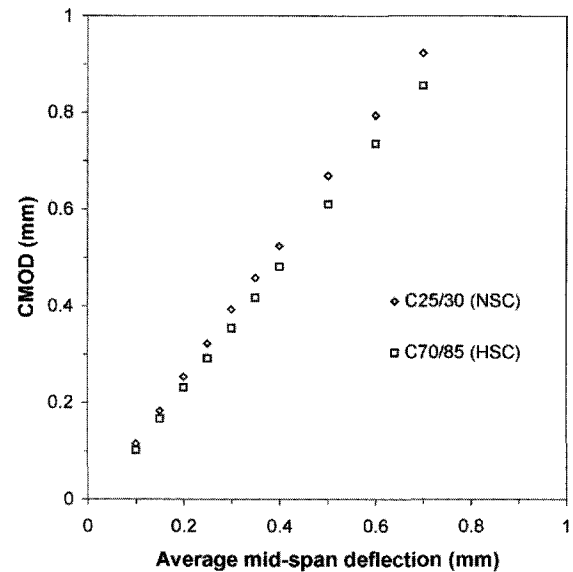


Fig. 11 – Relationship between CMOD and  $\delta$  for plain concrete beams.

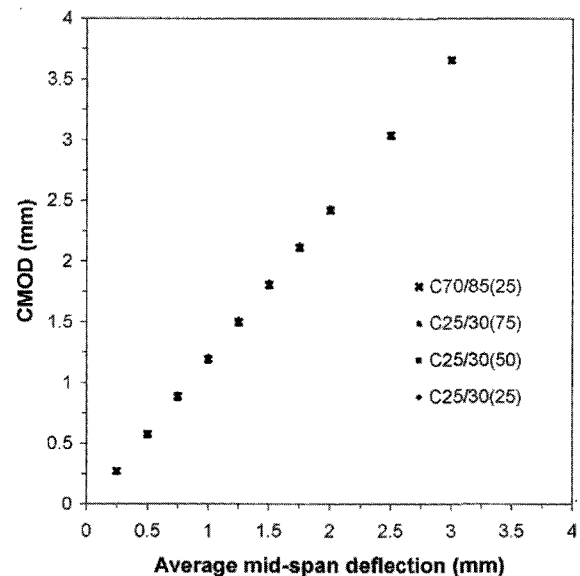


Fig. 12 – Relationship between CMOD and  $\delta$  for SFRC beams.

extremely good. The data points seem to lie on top of one another. Divergence between the first and second phase results is not obvious because the SFRC beam tests were loaded well into the post-peak region and thus would not be as sensitive to differences in  $d_o$  as that observed for the plain concrete beams.

Using the plain NSC beams as a benchmark from the previous study (refer to Section 4.3), Fig. 11 indicates that the relationship found between  $\delta$ -CMOD would also apply for the plain HSC through logical deduction (as the data points for both types of concrete are quite close with each other in Fig. 11). Similarly, it can be deduced from Fig. 12 that the relationship between CMOD and  $\delta$  not only holds for the C25/30 with 50kg/m<sup>3</sup> of fibres, but also applies to all the fibre concrete types considered.

Figs. 11 and 12 were plotted using the average values calculated using all the results available from the round robin test programme. The ratio of  $\delta/CMOD$  was compiled along with coefficients of variation to determine whether any

**Table 3 – Tabulated ratios of  $\delta$ /CMOD at various prescribed average mid-span deflections and their coefficients of variation for the plain concrete beams**

Concrete grade	Ratio of $\delta$ /CMOD at prescribed average mid-span deflections $\left(\delta = \frac{L}{4} \cdot \frac{1}{H}\right)$									
	0.1	0.15	0.2	0.25	0.3	0.35	0.4	0.5	0.6	0.7
C25/30	0.874 (9.00)	0.822 (6.43)	0.792 (5.04)	0.776 (4.08)	0.765 (4.34)	0.766 (3.78)	0.765 (3.80)	0.750 (6.37)	0.757 (4.34)	0.760 (4.33)
C70/85	0.987 (8.66)	0.902 (8.20)	0.867 (6.88)	0.859 (5.06)	0.849 (5.82)	0.840 (4.71)	0.832 (3.99)	0.820 (3.50)	0.816 (2.83)	0.818 (2.32)

Note: Figures in **bold** are the prescribed average mid-span deflections,  $\delta$ , in millimetres  
 Figures in brackets are the coefficients of variation, V (%)

**Table 4 – Tabulated ratios of  $\delta$ /CMOD at various prescribed average mid-span deflections and their coefficients of variation for the SFRC beams**

Concrete grade (Fibre dosage in kg/m <sup>3</sup> )	Ratio of $\delta$ /CMOD at prescribed average mid-span deflections $\left(\delta = \frac{L}{4} \cdot \frac{1}{H}\right)$									
	0.25	0.5	0.75	1.0	1.25	1.5	1.75	2.0	2.5	3.0
C25/30 (25)	0.917 (9.58)	0.856 (6.00)	0.833 (5.25)	0.828 (5.60)	0.824 (5.43)	0.823 (5.05)	0.822 (4.67)	0.821 (4.36)	0.822 (4.17)	0.823 (4.12)
C25/30 (50)	0.898 (7.15)	0.854 (5.62)	0.840 (5.44)	0.835 (5.31)	0.832 (5.35)	0.830 (5.34)	0.830 (5.68)	0.832 (5.10)	0.833 (4.82)	0.836 (4.88)
C25/30 (75)	0.969 (4.29)	0.894 (3.87)	0.865 (3.41)	0.851 (3.03)	0.843 (3.03)	0.837 (3.09)	0.833 (2.87)	0.829 (2.85)	0.828 (2.32)	0.824 (2.60)
C70/85 (25)	0.923 (10.8)	0.870 (7.16)	0.850 (5.39)	0.840 (4.47)	0.835 (3.93)	0.831 (3.63)	0.829 (3.65)	0.828 (3.55)	0.824 (3.28)	0.822 (3.10)

Note: Figures in **bold** are the prescribed average mid-span deflections,  $\delta$ , in millimetres  
 Figures in brackets are the coefficients of variation, V (%)

deviations from linearity was lost due to averaging. Tables 3 and 4 show the ratio of  $\delta$ /CMOD at various average mid-span deflections for the plain concrete and SFRC beams respectively. It is clear that the coefficients of variation, V, for all the values considered are below 10%. Furthermore, the majority of the variations are within 5%. This suggests that the linear relationship would not solely be applicable to the averaged values, but would be applicable globally (for the test dimensions used in the round robin test programme).

## 5. INTERCHANGING BETWEEN $\delta$ AND CMOD

To study the impact of interchanging between  $\delta$  and CMOD using the proposed simple model, the round robin beam results were re-analysed by converting CMOD values into equivalent  $\delta$  values. This was achieved using the expression:

$$\delta_e = \frac{L}{4} \cdot \frac{1}{H} \cdot \text{CMOD} \quad (3)$$

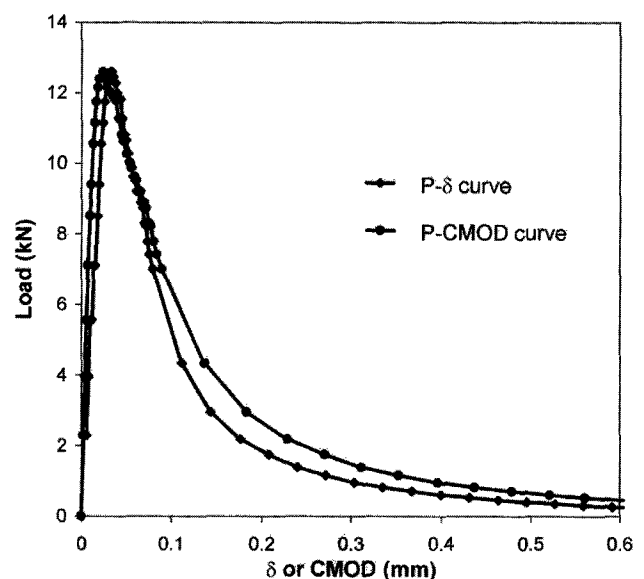
where,  $\delta_e$  = equivalent mid-span deflection, L = span at which the beam is tested, H = the apparent depth about which the beam rotates and CMOD = nominal (or measured) CMOD.

The P- $\delta$  curves for the beam specimens were converted to P- $\delta_e$  curves using Equation (3). Typical curves for a plain concrete beam are shown in Figs. 13 and 14.

By converting the CMOD values to equivalent mid-span deflection values ( $\delta_e$ ), the agreement between the P- $\delta$  and

P-CMOD curves (Fig. 13) is improved (Fig. 14). This is especially true where the post-peak regime is concerned. The difference between the two curves in the initial part of the curves is actually increased, but this increase is not seen as substantial. The application of Equation (3) has the effect of shifting the P-CMOD towards the left in a linear fashion because the abscissa values are reduced by a factor. This factor is a function of the apparent depth about which the beam rotates, H.

Figs. 15 and 16 show the impact of the conversion from the P-CMOD curve to the P- $\delta_e$  curve for a typical SFRC beam. As the SFRC specimens are tested for a relatively

Fig. 13 – P- $\delta$  and P-CMOD curves for a typical plain NSC beam.



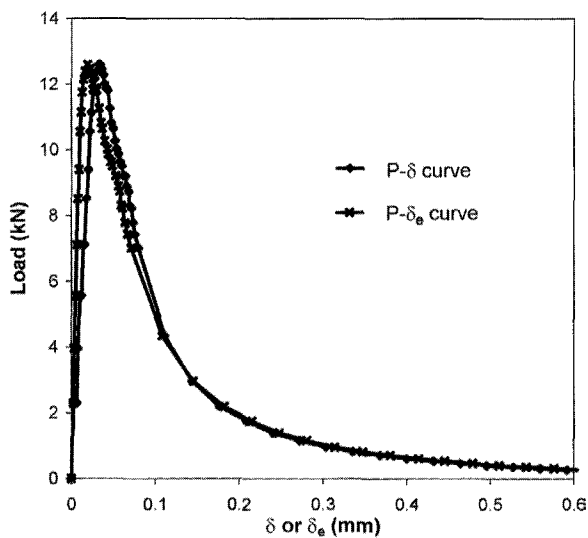


Fig. 14 – P-δ and P-δ<sub>e</sub> curves for a typical plain NSC beam.

long time as compared to the plain beams, the agreement between the P-δ and P-δ<sub>e</sub> curves is greater. Similarly, the difference between the two curves in the initial part of the curves is increased but not significantly so.

To have a quantitative evaluation of the impact of the conversion, loads at prescribed mid-span deflections were obtained from both the P-δ and P-δ<sub>e</sub> curves. This was carried out for both the plain and SFRC specimens. The difference between the loads obtained from the two curves is quantified using the expression:

$$\Delta D = \left| \frac{P_{\delta_e} - P_{\delta}}{P_{\delta}} \right| \times 100\% \quad (4)$$

where, ΔD = difference between the load obtained from the P-δ and P-δ<sub>e</sub> curves at a particular prescribed mid-span deflection, P<sub>δ<sub>e</sub></sub> = the load evaluated from the P-δ<sub>e</sub> curve and P<sub>δ</sub> = the load evaluated from the P-δ curve

Tables 5a and 5b show the results calculated for the plain

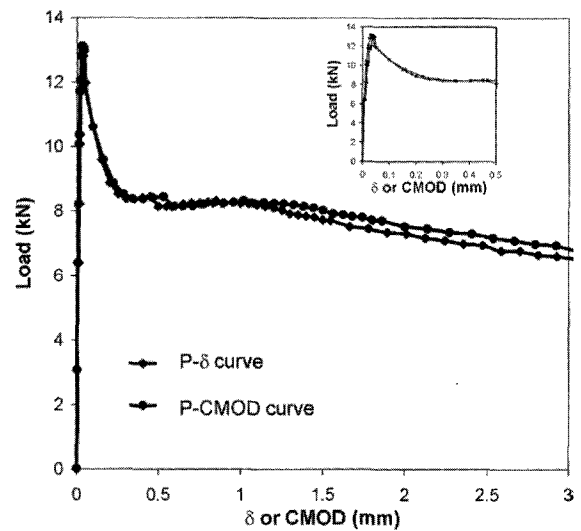


Fig. 15 – P-δ and P-CMOD curves for a C25/30 with 25kg/m<sup>3</sup> of fibres (Dramix 65/60 BN) SFRC beam.

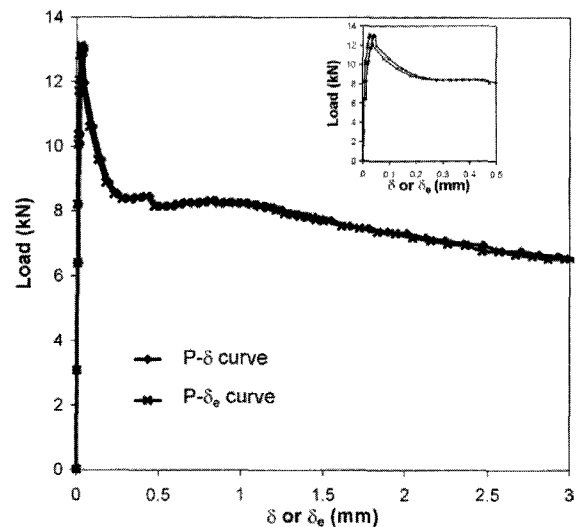


Fig. 16 – Typical P-δ and P-δ<sub>e</sub> curves for a C25/30 with 25kg/m<sup>3</sup> of fibres (Dramix 65/60 BN) SFRC beam.

Table 5a – Comparison between the loads obtained from the P-δ and P-δ <sub>e</sub> curves at various mid-span deflections for the plain NSC beams						
Curve	Load at prescribed mid-span deflections (kN)					
	0.1	0.15	0.2	0.25	0.3	0.4
P-δ	5.38	3.30	2.19	1.56	1.14	0.662
V(%)	(15.6)	(20.0)	(23.4)	(25.5)	(27.9)	(33.2)
P-δ <sub>e</sub>	4.86	3.14	2.17	1.60	1.17	0.709
V(%)	(15.0)	(18.9)	(21.9)	(24.1)	(28.3)	(30.6)
ΔD(%)	9.56	4.96	0.563	2.49	3.22	7.16

Note: Figures in **bold** denote the prescribed mid-span deflections in millimetres (mm)

Figures in brackets are the coefficients of variation, V(%)

Table 5b - Comparison between the loads obtained from the P-δ and P-δ <sub>e</sub> curves at various mid-span deflections for the plain HSC beams						
Curve	Load at prescribed mid-span deflections (kN)					
	0.1	0.15	0.2	0.25	0.3	0.4
P-δ	5.39	2.67	1.68	1.13	0.801	0.470
V(%)	(17.3)	(17.9)	(21.2)	(23.6)	(24.3)	(32.8)
P-δ <sub>e</sub>	4.17	2.35	1.54	0.985	0.745	0.441
V(%)	(18.1)	(21.3)	(24.5)	(26.9)	(24.9)	(34.9)
ΔD(%)	22.6	11.9	8.18	13.2	6.95	6.24

Note: Figures in **bold** denote the prescribed mid-span deflections in millimetres (mm)

Figures in brackets are the coefficients of variation, V(%)

NSC and HSC beams respectively. The difference, ΔD, is generally within 10% indicating a satisfactory agreement between the P-δ and P-δ<sub>e</sub> curves for the mid-span deflections considered.

Tables 6a to 6d show the results obtained for the SFRC beams. The agreement between the P-δ and P-δ<sub>e</sub> curves is

excellent for the mid-span deflections considered with the difference, ΔD, below 5%.

In addition, the variations at the prescribed mid-span deflections have been plotted and a comparison made between those obtained from the P-δ curve and from the P-δ<sub>e</sub> curve. Figs. 17 and 18 show such a comparison for the plain concrete specimens. Similarly, Figs. 19 and 20 show

the comparison for the SFRC beams. In general, the variation does not change significantly when the P- $\delta$  curve is transformed into the P- $\delta_e$  curve using the proposed simple rigid body model. This is true for both the plain and SFRC beams.

**Table 6a - Comparison between the loads obtained from the P- $\delta$  and P- $\delta_e$  curves at various mid-span deflections for the C25/30 (with 25kg/m<sup>3</sup> of Dramix 65/60 BN fibres) SFRC beams**

Curve	Load at prescribed mid-span deflections (kN)					
	0.5	1.0	1.5	2.0	2.5	3.0
P- $\delta$	7.75	7.54	7.31	6.98	6.60	6.33
V(%)	(24.3)	(26.7)	(27.6)	(28.2)	(28.8)	(29.6)
P- $\delta_e$	7.85	7.65	7.39	7.00	6.61	6.31
V(%)	(25.3)	(27.9)	(28.5)	(28.9)	(29.5)	(30.1)
$\Delta D$ (%)	1.29	1.49	1.07	0.413	0.219	0.197

Note: Figures in **bold** denote the prescribed mid-span deflections in millimetres (mm)

Figures in brackets are the coefficients of variation, V(%)

**Table 6b - Comparison between the loads obtained from the P- $\delta$  and P- $\delta_e$  curves at various mid-span deflections for the C25/30 (with 50kg/m<sup>3</sup> of Dramix 80/60 BN fibres) SFRC beams**

Curve	Load at prescribed mid-span deflections (kN)					
	0.5	1.0	1.5	2.0	2.5	3.0
P- $\delta$	16.5	18.0	18.2	17.8	17.0	16.6
V(%)	(22.5)	(21.9)	(22.2)	(22.9)	(22.9)	(22.8)
P- $\delta_e$	16.6	18.0	18.2	17.7	16.8	16.4
V(%)	(22.2)	(21.9)	(22.3)	(23.2)	(23.1)	(23.1)
$\Delta D$ (%)	0.581	0.299	0.147	0.764	0.967	1.20

Note: Figures in **bold** denote the prescribed mid-span deflections in millimetres (mm)

Figures in brackets are the coefficients of variation, V(%)

**Table 6c - Comparison between the loads obtained from the P- $\delta$  and P- $\delta_e$  curves at various mid-span deflections for the C25/30 (with 75kg/m<sup>3</sup> of Dramix 65/60 BN fibres) SFRC beams**

Curve	Load at prescribed mid-span deflections (kN)					
	0.5	1.0	1.5	2.0	2.5	3.0
P- $\delta$	20.0	20.4	19.8	18.9	18.0	17.3
V(%)	(14.9)	(16.0)	(16.9)	(16.8)	(15.5)	(15.0)
P- $\delta_e$	19.9	20.1	19.5	18.4	17.6	16.7
V(%)	(14.7)	(14.9)	(16.2)	(15.5)	(13.9)	(14.6)
$\Delta D$ (%)	0.127	1.39	1.88	2.47	2.07	3.18

Note: Figures in **bold** denote the prescribed mid-span deflections in millimetres (mm)

Figures in brackets are the coefficients of variation, V(%)

**Table 6d - Comparison between the loads obtained from the P- $\delta$  and P- $\delta_e$  curves at various mid-span deflections for the C70/85 (with 25kg/m<sup>3</sup> of Dramix 80/60 BP fibres) SFRC beams**

Curve	Load at prescribed mid-span deflections (kN)					
	0.5	1.0	1.5	2.0	2.5	3.0
P- $\delta$	13.2	15.6	16.8	17.3	17.2	16.7
V(%)	(30.1)	(30.7)	(31.4)	(31.5)	(31.2)	(31.9)
P- $\delta_e$	13.2	15.5	16.5	17.0	16.9	16.5
V(%)	(25.5)	(25.5)	(26.7)	(26.8)	(26.4)	(26.1)
$\Delta D$ (%)	0.171	1.10	1.84	1.86	1.96	1.43

Note: Figures in **bold** denote the prescribed mid-span deflections in millimetres (mm)

Figures in brackets are the coefficients of variation, V(%)

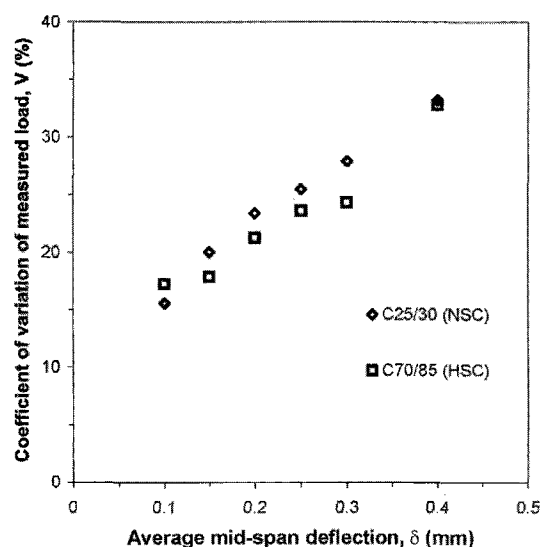


Fig. 17 – Variation of measured load at prescribed average mid-span deflections,  $\delta$  (variation obtained from P- $\delta$  curves) for the plain concrete beams.

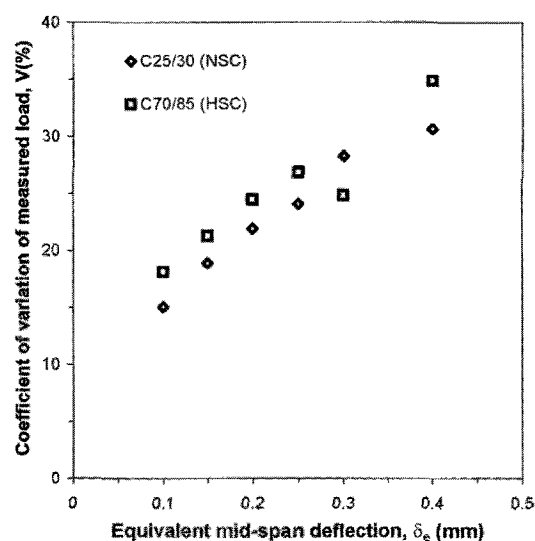


Fig. 18 – Variation of measured load at equivalent mid-span deflections,  $\delta_e$  (variation obtained from P- $\delta_e$  curves) for the plain concrete beams.

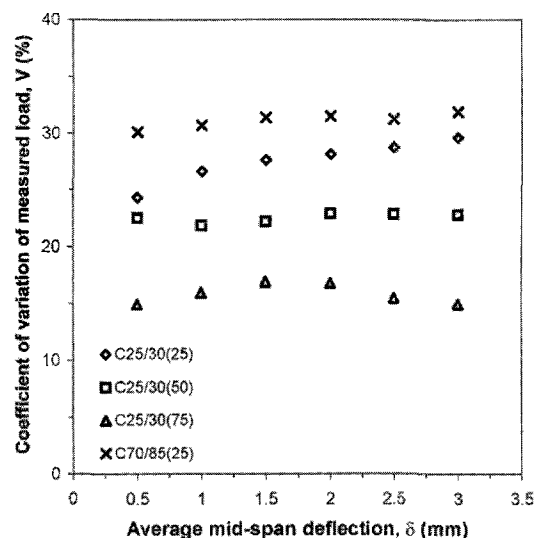


Fig. 19 – Variation of measured load at prescribed average mid-span deflections,  $\delta$  (variation obtained from P- $\delta$  curves) for the SFRC beams.

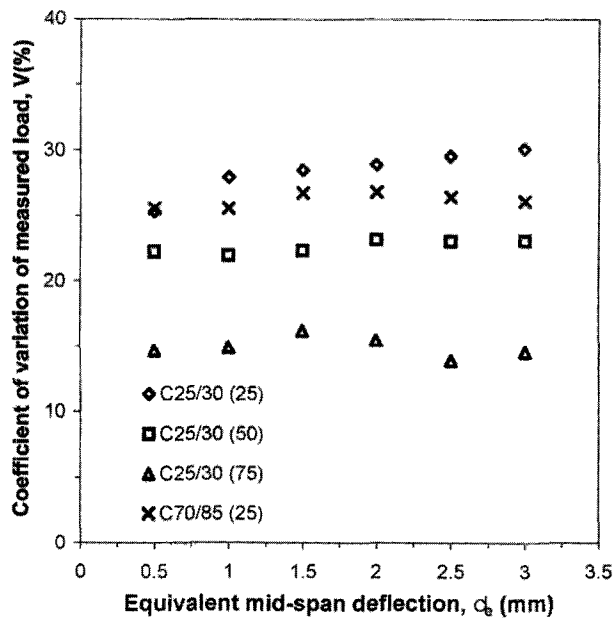


Fig. 20 – Variation of measured load at equivalent mid-span deflections,  $\delta_e$  (variation obtained from P- $\delta_e$  curves) for the SFRC beams.

In summary, it is found that the simple rigid body model is appropriate for converting the P-CMOD curve into a P- $\delta_e$  curve. The P- $\delta_e$  curve is found to agree well with the experimentally obtained P- $\delta$  curve, especially for the SFRC beams.

It is therefore suggested that the P-CMOD curve be used to obtain design parameters rather than the P- $\delta$  curve. This will facilitate the possibility of measuring CMOD alone to obtain the parameters using a simple relationship between  $\delta$  and CMOD as given by Equation (3) and thus save set-up time and cost. This simple relationship should be used to obtain a correction factor to interchange between  $\delta$  and CMOD (for example for a knife edge thickness,  $d_0 = 5\text{mm}$ , the ratio of  $\delta_e/\text{CMOD} = 0.8065$ ). This method can be used to either evaluate toughness or residual strengths using the P-CMOD curve.

## 6. CONCLUSIONS

The study reported here shows that there would be a certain amount of error with regard to different values of  $d_0$  being used when conducting a beam-bending test. The amount of error introduced in general increases as  $d_0$  increases. From the analytical analysis, for an error level of 10%, a knife-edge of 5mm would be acceptable. Bearing in mind the variation due to the distribution of fibres a knife edge thickness of 5mm is thus recommended. This value was chosen as a compromise between accuracy of measurement and practical considerations (especially for practising engineers).

The accuracy of a proposed model, based on rigid body kinematics, to obtain a relationship between  $\delta$  and CMOD was investigated. Analysis was carried out using both experimental and analytical results. In both plain and SFRC beams, it was found that there was close agreement between the model and the experimental and analytical results. Another study conducted showed that this relationship between  $\delta$  and CMOD was independent of the fibre contents and the concrete strengths considered. Furthermore, P-CMOD curves were converted into

P- $\delta_e$  curves using the simple rigid body model. This was found to be in close agreement with the experimentally measured P- $\delta$  curve especially for the SFRC beams.

The results show that toughness can be evaluated from either the P- $\delta$  or P-CMOD curves. With the support of both analytical and experimental evidence, it is recommended that the P-CMOD curve be used for evaluating the toughness or residual strengths of SFRC. However, the relationship between P- $\delta$  and P-CMOD needs to be established for any given geometry.

## ACKNOWLEDGEMENTS

The work reported in this paper forms part of the Brite-Euram project "Test and Design Methods for Steel Fibre Reinforced Concrete", contract no. BRPR-CT98-0813. The partners in the project are: N.V.Bekaert S.A. (Belgium coordinator), Centre Scientifique et Technique de la Construction (Belgium), Katholieke Universiteit Leuven (Belgium), Technical University of Denmark (Denmark), Balfour Beatty Rail Ltd (Great Britain), University of Wales Cardiff (Great Britain), Fertig-Decken-Union GmbH (Germany), Ruhr-University-Bochum (Germany), Technical University of Braunschweig (Germany), FCC Construcción S.A. (Spain), Universitat Politècnica de Catalunya (Spain).

## REFERENCES

- [1] RILEM TC 162-TDF, 'RILEM TC 162-TDF: Test and design methods for steel fibre reinforced concrete. Bending test, *Mater. Struct.* **33** (2000) 3-5.
- [2] Barr, B.I.G. and Lee, M.K., 'Definition of Round Robin Test. Preparation of Specimens. Execution and Evaluation of Round Robin Testing', Report from Test and Design Methods for Steel Fibre Reinforced Concrete, EU Contract – BRPR – CT98 – 813 (2001) 105 p.
- [3] Barr, B.I.G., Lee, M.K., de Place Hansen, E.J., Dupont, D., Erdem, E., Schaerlaekens, S., Schnütgen, S., Stang, H. and Vandewalle, L., 'Round robin analysis of the RILEM TC 162-TDF beam-bending test: Part 1 – Test method evaluation', *Mater. Struct.* **36** (263) (2003) 609-620.
- [4] RILEM TC 162-TDF, 'RILEM TC 162-TDF. Test and design methods for steel fibre reinforced concrete.  $\sigma$ - $\epsilon$  design method. Recommendations', *Mater. Struct.* **33** (226) (2000) 75-81.
- [5] Gopalaratnam, V.S., Shah, S.P., Batson, G.B., Criswell, M.E., Ramakrishnan, V. and Wecharatana, M., 'Fracture toughness of fiber reinforced concrete', *ACI Materials Journal* **88**(4) (1991) 339-353.
- [6] Gopalaratnam, V.S., Gettu, R., Carmona, S. and Jamet, D., 'Characterization of the toughness of fiber reinforced concretes using the load-CMOD response', in Proceedings FRAMCOS-2, edited by Wittmann, F.H., AEDIFICATIO Publishers, Freiburg (1995) 769-782.
- [7] Barr, B., Gettu, R., Al-Oraimi, S.K.A. and Bryars, L.S., 'Toughness measurement – the need to think again', *Cement and Concrete Composites* **18** (1996) 281-297.
- [8] Navalurkar, R.K., Hsu, T.T.C., Kim, S.K. and Wecharatana, M., 'True fracture energy of concrete', *ACI Materials Journal* **96**(2) (1999) 213-227.
- [9] Ferreira, L., Gettu, R. and Bittencourt, T., 'Study of Crack Propagation in the Specimen Recommended by RILEM TC 162-TDF Based on Linear Elastic Fracture Mechanics', Report from Test and Design Methods for Steel Fibre Reinforced Concrete, EU Contract – BRPR – CT98 – 813 (2001) 9p.
- [10] Stang, H., 'Analysis of 3-point bending test', Report from Test and Design Methods for Steel Fibre Reinforced Concrete, EU Contract – BRPR – CT98 – 813 (2001) 7p.